Inorganic Chemistry

Article

pubs.acs.org/IC

A Mononuclear Transition Metal Single-Molecule Magnet in a Nuclear Spin-Free Ligand Environment

Majed S. Fataftah,[†] Joseph M. Zadrozny,[†] Dylan M. Rogers, and Danna E. Freedman*

Department of Chemistry, Northwestern University, Evanston, Illinois 60208, United States

Supporting Information

ABSTRACT: The high-spin pseudotetrahedral complex $[Co(C_3S_5)_2]^{2-}$ exhibits slow magnetic relaxation in the absence of an applied dc magnetic field, one of a small number of mononuclear complexes to display this property. Fits to low-temperature magnetization data indicate that this single-molecule magnet possesses a very large and negative axial zero-field splitting and small rhombicity. The presence of single-molecule magnet behavior in a zero-nuclear spin ligand field offers the opportunity to investigate the potential for this molecule to be a qubit, the smallest unit of a quantum information processing (QIP) system. However, simulations of electron paramagnetic resonance (EPR) spectra and the absence of EPR spectra demonstrate that this molecule is unsuitable as a qubit due to the same factors that promote single molecule magnet behavior. We discuss the influence of rhombic and axial zero-field splitting on QIP applications and the implications for future molecular qubit syntheses.

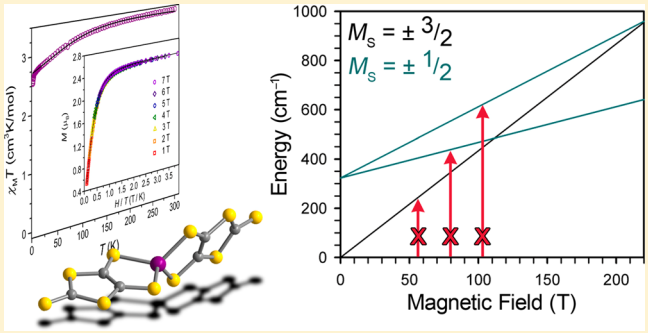

INTRODUCTION

Single molecule magnets (SMMs), or species displaying slow magnetic relaxation, exhibit a barrier to spin inversion due to magnetic bistability of two $\pm M_S$ levels.[1] This bistable magnetic ground state enables SMMs to behave as the analogues of permanent magnets, retaining their magnetization upon the removal of an applied magnetic field. While the first two decades of SMM research focused heavily on large polynuclear species of transition metals, in recent years, a number of mononuclear SMMs have been reported.[2] In these complexes, considerable axial zero-field splitting engenders magnetic bistability and slow magnetic relaxation in the absence of a high ground-state spin. Mononuclear SMMs offer significant synthetic tunability of zero-field splitting via variation of the coordination number and ligand field. The facile tunability of magnetic properties in mononuclear complexes may enable an oft-cited application for SMMs: quantum information processing (QIP).[3] Note that a significant amount of research into multi- and mononuclear molecular magnets has proceeded with the vision of using the spins in such complexes as the smallest logical unit of the QIP system, the qubit.[1,4,5] There exists a rich precedent in the physics literature of the viability of paramagnetic species as qubits through the observation of quantum coherence in the spins of such molecules.[6] The aforementioned tunability of the ligand fields in mononuclear SMMs is particularly attractive for QIP applications, since the afforded command of the zero-field splitting ensures control of the energies of electron paramagnetic resonance (EPR) transitions. As electronic spin-based QIP exploits EPR-accessible transitions for qubit manipulation, the frequently observed large axial zero field splittings in $S \geq {}^1/_2$ mononuclear systems are desirable since energetically separated transitions ensure selective qubit manipulation. However, evaluations of transition metal complexes with large-magnitude, negative axial zero-field splittings as qubit candidates are, to the best of our knowledge, absent in the literature. Herein, we report a mononuclear transition metal SMM with a very large, negative zero-field splitting and evaluate both its properties as a SMM and suitability as a qubit.

RESULTS AND DISCUSSION

To find a complex with the requisite geometry and electronic structure for a large negative zero-field splitting, we focused our attention upon pseudotetrahedral Co^{2+} complexes with two bidentate ligands with small bite angles. Inspection of the literature revealed the existence of the Co^{2+} complex, $(Ph_4P)_2[Co(C_3S_5)_2]$ (**1**) ($C_3S_5^{2-}$ = 4,5-dimercapto-1,3-dithiole-2-thione dianion; see Figure 1).[7,8] The structure of **1**, characterized by single-crystal X-ray diffraction, is comprised of a Co^{2+} center ligated by two nuclear spin-free bidentate sulfur-based ligands. The ∼94° bite angle of the $C_3S_5^{2-}$ ligand generates a tetragonally elongated pseudtotetrahedral coordination sphere and affords the splitting of the 3d orbitals depicted in Figure 1. This ligand field creates a near-degeneracy of the d_{xy} and $d_{x^2-y^2}$ orbitals (see Figure 1 and SI for details regarding the ligand field model), producing a low-lying d−d electronic excited state that yields a large and negative

Received: August 5, 2014
Published: September 8, 2014

   dx.doi.org/10.1021/ic501906z | *Inorg. Chem.* 2014, 53, 10716−10721

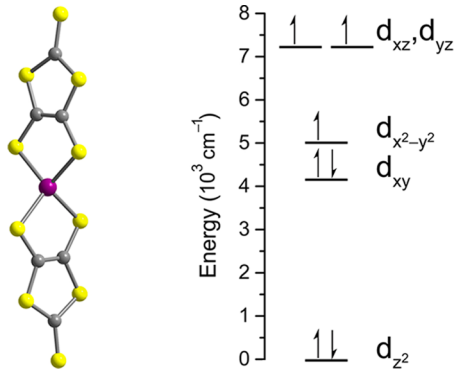

Figure 1. Left: Structure of $[Co(C_3S_5)_2]^{2-}$ in **1**. Purple, yellow, and gray spheres represent Co, S, and C atoms, respectively. Selected interatomic distances (Å) and angles (deg): Co−S 2.293(1)−2.3077(1), nearest Co···Co 8.6591(5), S−Co−S 94.047(4), 94.127(4), 100.605(4), 112.648(5), 123.483(4), 124.623(4); dihedral angle between approximate planes of the $C_3S_5^{2-}$ ligands, 79.3(2) and 100.7(2). Right: Approximate d-orbital energies and ground state electron configuration for **1**, as described in the main body of the report and SI.

contribution to the axial zero-field splitting (D) of the $S = {}^3/_2$ Co^{2+} ion.[2d,g] Analysis of the higher-energy d−d transitions expected for this electronic configuration reveal that the contributions to the transverse anisotropy (E) of excited states arising from transitions to the d_{xz} and d_{yz} orbitals are of opposing parity. Thus, the magnitude of E will be suppressed by a near-degeneracy of the d_{xz}, d_{yz} pair.[9] Indeed, if ideal D_{2d} molecular geometry were realized in **1**, a net zero magnitude of E would be achieved, as contributions to E from excited states involving the d_{xz} orbital will cancel contributions from the d_{yz} orbital. Thus, one may expect a large uniaxial magnetic anisotropy for **1** and a small transverse component, the latter on account of the observed deviation from pure D_{2d} symmetry.

To probe the magnetic anisotropy of **1**, magnetic susceptibility and magnetization data were acquired. The room temperature magnetic susceptibility, $\chi_M T$ = 3.24 cm^{3}K/mol, is consistent with an $S = {}^3/_2$ ground state and a g_{iso} value of 2.63 (see Figure 2). The large observed g_{iso} value is in accordance with literature values for structurally similar compounds with large magnetic anisotropies.[2d,g,10] With decreasing temperature, $\chi_M T$ remains constant until 120 K at

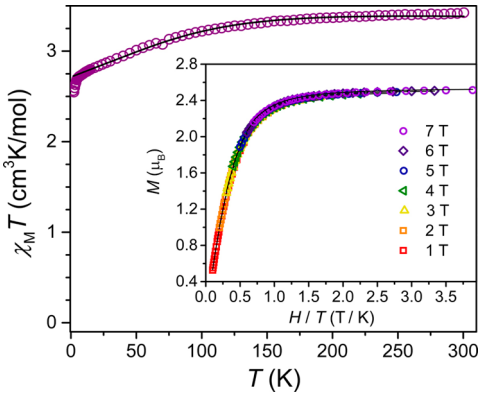

Figure 2. Variable-temperature dc susceptibility data for **1** with H_{dc} = 1 kOe. The black line is a best fit to the data with $g_{||}$ = 3.10, $g_{\perp}$ = 2.34, and $|D|$ = 127 cm^{-1}. Inset: Isofield lines for **1**; black lines represent the best fit with g_{iso} = 3.24, D = −161 cm^{-1}, and E = 0 cm^{-1}.

which point $\chi_M T$ monotonically decreases, ultimately reaching 2.2 cm^{3}K/mol at 1.8 K. This temperature dependence of $\chi_M T$ is further indicative of zero-field splitting and is typical of distorted tetrahedral Co^{2+} ions.[2d,g,10]

Quantitation of the magnetic anisotropy of **1** proceeded via the fitting of susceptibility and magnetization data acquired on powder samples (see Figures 2 and S2). We note the difficulty in obtaining accurate values of D and E from fitting of powder samples. Figure 2 depicts a fit to the dc susceptibility data with $\hat{H} = D\hat{S}_z^2 + g_{\perp}\beta\mathbf{SH} + g_{||}\beta\mathbf{SH}$ and the Van Vleck equation,[11] where D is the axial zero field splitting, $\hat{S}_z$ is the z-component spin operator, $g_{\perp}$ and $g_{||}$ are the perpendicular and parallel components of the g factor, respectively, β is the Bohr magneton, **S** is the spin, and **H** is the applied dc field, and the implicit assumption here is a zero E. A second estimation of the large magnitude of D was obtained by fitting the low temperature magnetization data (see Figure 2 inset) with ANISOFIT 2.0[12] and the Hamiltonian $\hat{H} = D\hat{S}_z^2 + E(\hat{S}_x^2 - \hat{S}_y^2) + g_{iso}\beta\mathbf{SH}$. Here, E is the transverse anisotropy, $\hat{S}_x$ and $\hat{S}_y$ are spin operators, while g_{iso} represents an isotropic g factor, and the other parameters retain their previous definitions. We attribute much of the variation between the obtained sets of parameters in our fits to the differing assumptions implicit in each of the Hamiltonians. However, our results consistently estimate D to be between −100 and −200 cm^{-1} (see SI for additional fits and discussion), while E is estimated to be very small. In the context of other reports, any of the D values reported here are close to the largest negative values of D spectroscopically observed in other mononuclear transition metal complexes.[13]

The hallmark of a SMM is frequency dependent magnetic relaxation enforced by a barrier to spin reversal. The fits of the dc data suggest that a substantial spin reversal barrier exists in **1** on account of the relative stability of the $M_S = \pm{}^3/_2$ levels to the $\pm{}^1/_2$ levels. To verify this prediction, variable-frequency ac susceptibility measurements were performed on **1** to search for slow magnetic relaxation (see Figures 3, S4−S10). Indeed, at zero applied dc field and 2 K, a peak is observed in the out-of-phase ac susceptibility (χ_M'') at 0.84 Hz with a second smaller peak appearing at 220 Hz. With increasing temperature, the low-frequency peak rapidly moves toward higher frequencies, while the high frequency peak quickly decreases in intensity but remains at the same frequency (Figure 3). Application of a dc field at 2 K causes both the low- and high-frequency peaks to diminish while a new peak with a maximum below 0.1 Hz intensifies (see Figure S28). At 5 K, the peak fades into a growing peak at a lower frequency, 4.8 Hz, and the effect appears to saturate at H_{dc} = 1000 Oe (see Figure S10).

Analysis of the temperature dependence of τ was conducted to determine the process responsible for the slow magnetic relaxation.[14] Notably, relaxation via quantum tunneling[15] or avalanche[16] mechanisms can provide temperature-independent relaxation times, which are observed in **1** below 3 K. Above 3 K, however, τ is highly temperature dependent. In mononuclear SMMs, such temperature dependence is most often correlated to Raman and Orbach spin reversal processes. The former imparts a T^n dependence on τ, while the latter is exponential. Importantly, the Orbach process requires quantized energy exchange with the lattice via excitations to higher-energy spin sublevels and thus directly invokes the concept of an energy barrier to spin reversal. In this latter case, a plot of $\ln(\tau)$ versus $1/T$ yields a straight line, where the slope corresponds to the effective magnitude of the spin reversal barrier, U_{eff}, and the y

dx.doi.org/10.1021/ic501906z | Inorg. Chem. 2014, 53, 10716−10721

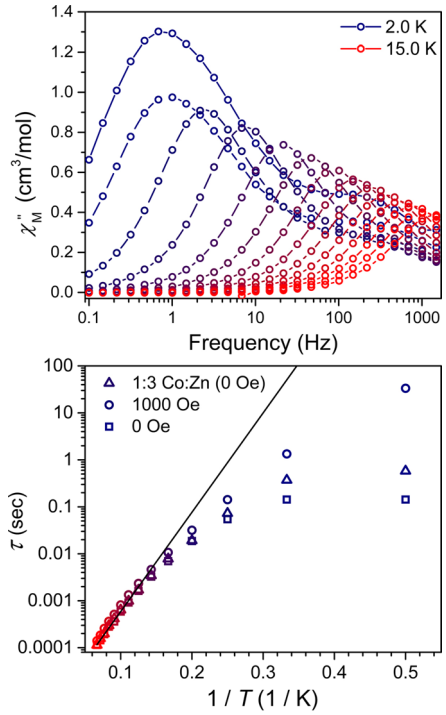

Figure 3. Top: Frequency dependence of the out of phase ac susceptibility of complex **1** under 0 Oe dc field from 2 to 15 K in increments of 1 K. Bottom: Arrhenius plots for **1** under 0 (squares) and 1000 Oe dc fields (circles) and dilute in a matrix of $(Ph_4P)_2[Zn(C_3S_5)_2]$ under 0 Oe dc field (triangles). Black lines represent a best fit to the data between 11 and 15 K to yield U_{eff} = 33.9 cm^{-1} and $\tau_o = 4.5 \times 10^{-6}$ s.

intercept corresponds to the attempt time, τ_o. For **1**, a linear fit to the H_{dc} = 0 Oe data between 11 and 15 K quantitates these parameters as U_{eff} = 33.9 cm^{-1} and $\tau_o = 4.5 \times 10^{-6}$ s. Importantly, the fit is nearly invariant when a dc field is applied to **1** (U_{eff} = 39.9 cm^{-1} and $\tau_o = 2.8 \times 10^{-6}$ s) or upon dilution in a diamagnetic matrix of $(Ph_4P)_2[Zn(C_3S_5)_2]$ (U_{eff} = 39.0 cm^{-1} and $\tau_o = 3.1 \times 10^{-6}$ s; see Figure 3 and SI). These values are similar to other known tetrahedral Co^{2+} SMMs,[2d,g] and on the basis of the dilution results we conclude that the slow magnetic relaxation in **1** is molecular in nature and not a bottleneck or collective process.[17] Thus, **1** is a member of a small subset of transition metal complexes that show slow magnetic relaxation at zero dc field[2d,e,g−i] and is the first to do so with the support of a ligand set that is nuclear spin-free.

Note that at low temperature, the relaxation time of **1** is 2 orders of magnitude slower than the similar species $(Ph_4P)_2[Co(SPh)_4]$[2d,g] despite stronger dipolar interactions on account of closer Co···Co distances (≈ 2 Å) and collinear molecular axes in the crystal structure. The relative slowing of τ in **1** at the lowest temperatures is likely owing to the differing coordination geometries between the two species. We note the nuclear spin-free ligand set of **1**, which may play a role in the low-temperature magnetization dynamics, as has been invoked for other SMMs.[18] However, **1** is not rigorously nuclear spin-free on account of the Ph_4P^+ protons and ^{31}P and ^{59}Co nuclei. Although it is more difficult to comment on the influence of the Ph_4P^+ nuclear spins on the magnetization dynamics at this stage, a recent report[19] has suggested a prominent role for the $I = {}^7/_2$ ^{59}Co nucleus in the magnetization dynamics of Co^{2+} complexes with positive D values. Note, however, that the role of such spins on quantum tunneling of the magnetization in systems with $D < 0$ is unexplored and represents a future topic of interest. The relative magnitude of the high frequency peak to the low frequency peak at zero dc field for **1** is consistent between multiple sample preparations, suggesting that the smaller peak is intrinsic to **1** and not arising from an impurity. However, the peak disappears both with an applied dc field as well as dilution (see Figures S10 and S11), and on this basis we tentatively attribute the high-frequency peak to a collective origin. The stark disagreement between the predicted 2D splitting by ANISOFIT (−322.8 cm^{-1}) and U_{eff} is notable and has been observed in similar species.[2d,g] The discrepancy may be partially attributed to vibronic coupling, which would lead to barrier reduction.[20] Although unlikely on account of the consistency between fits, the magnitude of D may be severely overestimated, and thus we expect an unreasonably large U_{eff}; however, it is far more likely that the high-temperature relaxation is erroneously assigned as an Orbach process, which is a common problem in the literature, as recently highlighted in refs 5e and 21. Thus, direct correlation of the value of U_{eff} reported here with the electronic structure of **1** should proceed with caution. This latter conclusion is further evidenced by the large value of τ_o obtained from the Arrhenius plot fitting. Definitive resolution of this ambiguity is not trivial. Ac susceptibility analysis at high temperatures is one route to reach pure thermally activated relaxation and would aid with the small range of data fit; however, at such temperatures, the τ values will have moved past the accessible frequency range of our magnetometer. In specific cases,[22] spectroscopic techniques have revealed pure thermally activated spin reversal in mononuclear single-molecule magnets. Note that the cited techniques, Mössbauer spectroscopy and NMR, are unsuitable for **1** on account of the nonferrous nuclei and absence of suitable NMR handles in the main body of the molecule.

Attempts to obtain continuous-wave and pulsed EPR spectroscopic data on **1** to probe the low-lying spin states were unsuccessful. Under a variety of conditions (see Experimental Section), both types of measurements elicited no signals. On the basis of the EPR silence, ac susceptibility data and magnetization data, we assign D as large and negative, though an exact value cannot be determined. Importantly, field-induced slow magnetic relaxation has precedent in mononuclear Co^{2+} complexes with positive D values, but none have shown the phenomenon at zero dc field.[23] We further note that on the basis of the relationship between U and D for a half-integer spin, $U = (S^2 - {}^1/_4)|D|$, the D apparent from the Arrhenius plot fit is approximately 17 cm^{-1}, which would have elicited a signal under the conditions in which we conducted our EPR investigation.

The absence of an EPR signal led us to carefully revisit our parameters determined by magnetometry. Note that these data imply an unusually large zero-field splitting and a negligible rhombic splitting. Data simulations employing g_{iso} = 3.24, D = −161 cm^{-1}, and E = 0 cm^{-1} obtained from magnetization data readily explain the EPR silence (Figure 4). The absence of an intra-Kramers transition of the $M_S = \pm{}^1/_2$ doublet is attributable primarily to the large D and subsequently small thermal population of that doublet at the temperature ranges of investigation. In fact, at that energy scale, a temperature of ∼200 K would be required to thermally populate (∼10%) the doublet and instill transition intensity. Alternatively, the inter-Kramers transition from the $M_S = \pm{}^3/_2$ to $M_S = \pm{}^1/_2$ doublet would become accessible to commercial frequencies only in dc

dx.doi.org/10.1021/ic501906z | Inorg. Chem. 2014, 53, 10716−10721

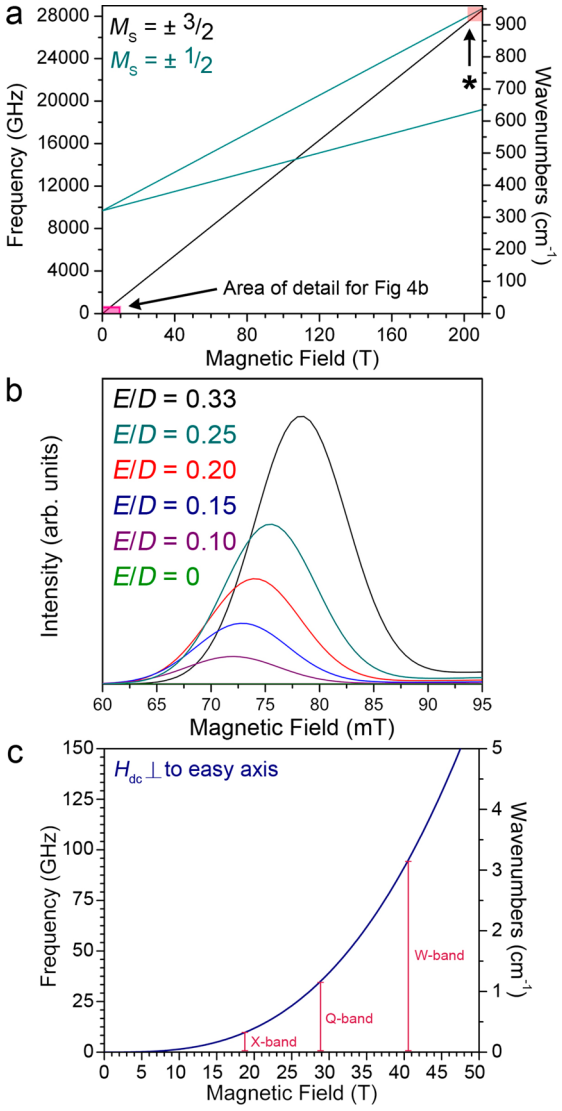

Figure 4. (a) Calculated Zeeman splitting diagram for an $S = {}^3/_2$ system with $g_{iso} = 3.24$, $D = -161$ cm^{-1}, $E = 0$ cm^{-1}, and H_{dc} applied along the easy axis. Energies are normalized to the ground $-{}^3/_2$ M_S level, which follows the x axis of the graph. *Field where inter-Kramers transition would be feasible, if thermal population permitted. (b) Intensity of the z-component of the intra-Kramers absorption of the $M_S = \pm{}^3/_2$ doublet at 9.735 GHz as a function of increasing rhombicity E/D for a powder with $g_{iso} = 3.24$ and $D = -161.4$ cm^{-1}. (c) Simulation of the energy of the $M_S = \pm{}^3/_2$ inter-Kramers transition as a function of applied field strength perpendicular to the easy axis. Vertical red lines indicate the expected fields of transitions at the frequencies of common commercial instruments. Note these fields are not attainable on such instruments.

fields that are over 4 times the world record ~45 T dc field achieved at the National High Magnetic Field Laboratory (see Figure 4a, S17). Even if those fields were attainable, both low thermal population and small population differences between states would prevent observation. Spectral simulations reveal the possibility of observing a formally forbidden transition within the $M_S = \pm{}^3/_2$ doublet (see Figure 4). Here, a nonzero E term relaxes the selection rule for the ground state transition and allows its observation at low field with low irradiation frequency, as shown in Figure 4b. The fact that no signal is observed for **1** may therefore be indicative of small transverse anisotropy. A separate route toward observation of the forbidden resonance entails application of a dc field in the hard plane of the Co^{2+} moment. Here, observation of the inter-Kramers transition is possible;[13] however, the fields required to observe these transitions are greater than fields currently available in any commercial instrument. Together, these simulations account for the complete EPR silence of this molecule and indicate why **1** is unsuitable as a qubit, as the absence of an observable, addressable spin transition prohibits the observation of a superposition by pulsed EPR. The optimal qubit system, in contrast to the ideal SMM, requires addressable transitions, though not necessarily forbidden ones. Thus, successful qubits can be realized in systems with significant E values and small D values (either positive or negative). These parameters compromise the existence and magnitude of a spin reversal barrier but instead afford utility for QIP. In this regard, we note the demonstration of coherent spin dynamics by certain species with small zero field splittings or low total S.[4,24]

CONCLUSIONS AND OUTLOOK

The foregoing results highlight a discord between the design criteria of mononuclear transition metal single-molecule magnets and molecules for spin-based quantum computation. Notably, it appears that successful qubit design requires the ability to rationally tune E, and our future research is focused in this new design direction.

EXPERIMENTAL SECTION

General. Manipulations of all compounds were performed under a dinitrogen atmosphere. Solvents were dried using a commercial solvent purification system from Pure Process Technology and stored over 3 or 4 Å sieves prior to use. Deuterated solvents were purchased from Cambridge Isotope Laboratories, deoxygenated by three successive freeze–pump–thaw cycles. $CoCl_2$ was prepared from $CoCl_2 \cdot 6H_2O$ following the method of Horvath as applied for preparation of $MnCl_2$.[25] 4,5-Bis(benzoylthio)1,3-dithiole-2-thione (benzoyl dmit) and 4,5-dimercapto-1,3-dithiol-2-thione disodium salt ($Na_2C_3S_5$) were prepared by the literature methods.[26,27] Crystal structures of **1** and **2** with different crystallizing solvents than previously reported were obtained for precise measurements of the bond distances and angles.[8,28] All other chemicals were used as received.

*Synthesis of $(Ph_4P)_2[Co(C_3S_5)_2]\cdot(MeCN)$ (**1**·(MeCN)).* A total of 230 mg of NaOMe was combined with 852 mg of benzoyl dmit in 10 mL of MeOH and was allowed to stir for 1 h, followed by the addition of 138 mg of $CoCl_2$ and 822 mg of $(Ph_4P)Br$. The mixture is stirred for an additional hour, filtered, washed with Et_2O, and then recrystallized from hot acetonitrile as dark red plates. Spectroscopic data matched previously reported values.[8] Anal. Calcd for $C_{54}H_{40}P_2S_{10}Co\cdot CH_3OH$: 56.82%C; 3.81%H. Found: 56.82%C; 3.78%H.

*Synthesis of $(Ph_4P)_2[Zn(C_3S_5)_2]\cdot(MeCN)$ (**2**·(MeCN)).* A total of 249 mg of $Na_2(C_3S_5)$ and 70 mg of $ZnCl_2$ were stirred in 10 mL of MeOH overnight, followed by the addition of 431 mg of $(Ph_4P)Br$. The mixture was allowed to stir for 1 h, filtered, washed with Et_2O, and then recrystallized from hot acetonitrile to yield dark red crystalline blocks. Anal. Calcd For $C_{54}H_{40}P_2S_{10}Zn\cdot CH_3CN$: 57.09%C; 3.69%H; 1.19%N. Found: 56.91%C; 3.52%H; 1.22%N.

*Synthesis of $(Ph_4P)_2[Zn_{0.67}Co_{0.33}(C_3S_5)_2]\cdot(MeCN)$ (**1′**·(MeCN)).* A total of 67 mg of **1** and 120 mg of **2** were codissolved in 20 mL of hot MeCN and rapidly cooled in a freezer held at −35.0 C to yield crystals of complex **1′** (155.2 mg). Single crystal X-ray analysis yielded the same unit cell as that collected for **1** ($a = 9.5656(5)$ Å, $b = 16.9629(9)$ Å, $c = 19.161(1)$ Å, $\alpha = 64.722(3)°$, $\beta = 78.283(3)°$, $\gamma = 77.780(3)°$, $V = 2722.85(6)$ Å^3).

Magnetic Measurements. Magnetic data were collected using a Quantum Design MPMS-XL SQUID magnetometer. Measurements

dx.doi.org/10.1021/ic501906z | Inorg. Chem. 2014, 53, 10716−10721

for **1** and **1′** were obtained on finely ground microcrystalline powders restrained in a frozen eicosane matrix and flame-sealed in a quartz tube or wrapped tightly within a polyethylene bag. In this latter case, the sample was transferred to the SQUID in a Schlenk flask under a constant flow of argon. Dc susceptibility measurements were collected in the temperature range 2−300 K under a dc field of 1000 Oe. Dc magnetization measurements were obtained in the temperature range 1.8−10 K under dc fields of 1−7 T in 1 T increments. Ac susceptibility measurements were obtained with a 4 Oe ac field oscillating at frequencies of 0.1−1488 Hz under various applied dc fields and temperatures. Dc magnetic susceptibility data were corrected for diamagnetic contributions from the sample holder and eicosane as well as for the core diamagnetism of each sample. The core diamagnetism was estimated to be -643×10^{-6} emu/mol for **1** and -648×10^{-6} emu/mol for **2** using Pascal's constants.[29] Prior to full characterization, magnetization versus applied dc field curves from 0 to 4 T were collected for each sample to ensure the absence of curvature associated with ferromagnetic impurities (see Figure S1). Data agreement was checked over multiple measurements. Note that two additional fits, depicted in Figure S3, truncate the full magnetization set by eliminating the 1 T data (Figure S3, top) and 1 and 2 T data (Figure S3, bottom). We performed fits on truncated data sets to ensure that the large magnitude, negative D values we observed were not local minima as a result of the range of fitted data.

X-ray Diffraction. Single crystal diffraction data collections were performed on single crystals coated with Paratone-N oil and mounted on a MicroMounts rod. The crystals were frozen under a stream of N_2 during measurements. Data were collected with a Bruker MICRO-STAR X-ray source of Mo Kα (λ = 0.71073 Å) radiation and a Bruker APEX-II detector. Raw data were integrated and corrected for Lorentz and polarization effects using Bruker Apex2 v. 2013.2.[30] Absorption corrections were applied using SADABS.[31] Space group assignments were determined by examination of systematic absences, E-statistics, and successive refinement of the structures. The crystal structure was solved by direct methods with the aid of successive difference Fourier maps in SHELXL[32] operated with the OLEX2 interface.[33] The crystals did not show significant decay during data collection. Thermal parameters were refined anisotropically for all non-hydrogen atoms in the main body, solvents of crystallization, and the Ph_4P^+ counterions. Hydrogen atoms were placed in ideal positions and refined using a riding model for all structures.

EPR Spectroscopy. Attempts to obtain EPR spectra were performed at the National High Magnetic Field Laboratory (NHMFL). Continuous-wave (CW) measurements were conducted on a broadband transmission spectrometer[34] with a 17 T superconducting magnet operating at frequencies of 50, 100, 150, 200, 300, and 400 GHz. Measurements were conducted at all the mentioned frequencies at temperatures of 4.2, 10, 20, 50, 77, and 300 K. Measurements were performed at various temperatures ranging from the lowest achievable at 4.2 K up to room temperature in attempts to populate the higher lying $M_s = \pm^1/_2$ states. Simulations of spectra as a function of D and E were performed with the program Easyspin.[35]

All Other Physical Measurements. Combustion analysis of **1** was performed by Midwest Microlab (Indianapolis, IN). Infrared spectra were recorded on a Bruker Alpha FTIR spectrometer equipped with an attenuated total reflectance accessory. Solution-phase NMR spectra were collected with an Agilent Au 400 MHz spectrometer. Proton NMR spectra are referenced to $CDCl_3$ at 7.26 ppm.

■ ASSOCIATED CONTENT

Ⓢ Supporting Information

Further discussion of the d-orbital splitting, spectroscopic characterization of **1** and **2**, ac and dc magnetic characterization, Cole−Cole plots, and Arrhenius fits are available. X-ray crystallographic information as CIFs. This material is available free of charge via the Internet at http://pubs.acs.org.

■ AUTHOR INFORMATION

Corresponding Author

*E-mail: danna.freedman@northwestern.edu.

Author Contributions

†These authors contributed equally to this work.

Funding

We are grateful for the financial support of Northwestern University and The Institute for Sustainability and Energy at Northwestern University (ISEN) Booster Award number 10031846. Work at the NHMFL is supported by the NSF (DMR1157490) and the State of Florida.

Notes

The authors declare no competing financial interest.

■ ACKNOWLEDGMENTS

We are grateful to Prof. Stephen Hill for invaluable discussions and insight regarding EPR experiments and simulations. We thank Ms. Lakshmi Bhaskaran for working to obtain EPR spectra. We also thank Dr. A. Ozarowski, Dr. L. Song, and S. Ling for the use of their EPR spectrometers and experimental assistance at the National High Magnetic Field Laboratory.

■ REFERENCES

(1) Gatteschi, D.; Sessoli, R.; Villain, J. *Molecular Nanomagnets*; Oxford University Press: Oxford, 2006.

(2) (a) Freedman, D. E.; Harman, W. H.; Harris, T. D.; Long, G. J.; Chang, C. J.; Long, J. R. *J. Am. Chem. Soc.* **2010**, *132*, 1224. (b) Harman, W. H.; Harris, T. D.; Freedman, D. E.; Fong, H.; Chang, A.; Rinehart, J. D.; Ozarowski, A.; Sougrati, M. T.; Grandjean, F.; Long, G. J.; Long, J. R.; Chang, C. J. *J. Am. Chem. Soc.* **2010**, *132*, 18115. (c) Weismann, D.; Sun, Y.; Lan, Y.; Wolmershauser, G.; Powell, A. K.; Sitzmann, H. *Chem.—Eur. J.* **2011**, *17*, 4700. (d) Zadrozny, J. M.; Long, J. R. *J. Am. Chem. Soc.* **2011**, *133*, 20732. (e) Mossin, S.; Tran, B. L.; Adhikari, D.; Pink, M.; Heinemann, F. W.; Sutter, J.; Szilagyi, R. K.; Meyer, K.; Mindiola, D. J. *J. Am. Chem. Soc.* **2012**, *134*, 13651. (f) Zadrozny, J. M.; Atanasov, M.; Bryan, A. M.; Lin, C.-Y.; Rekken, B. D.; Power, P. P.; Neese, F.; Long, J. R. *Chem. Sci.* **2013**, *4*, 125. (g) Zadrozny, J. M.; Telser, J.; Long, J. R. *Polyhedron* **2013**, *64*, 209. (h) Zhu, Y.-Y.; Cui, C.; Zhang, Y.-Q.; Jia, J.-H.; Guo, X.; Gao, C.; Qian, K.; Jiang, S.-D.; Wang, B.-W.; Wang, Z.-M.; Gao, S. *Chem. Sci.* **2013**, *4*, 1802. (i) Zadrozny, J. M.; Xiao, D. J.; Atanasov, M.; Long, G. J.; Grandjean, F.; Neese, F.; Long, J. R. *Nature Chem.* **2013**, *5*, 577. (j) Ishikawa, R.; Miyamoto, R.; Nojiri, H.; Breedlove, B. K.; Yamashita, M. *Inorg. Chem.* **2013**, *52*, 8300. (k) Martínez-Lillo, J.; Mastropietro, T. F.; Lhotel, E.; Paulsen, C.; Cano, J.; De Munno, G.; Faus, J.; Lloret, F.; Julve, M.; Nellutla, S.; Krzystek, J. *J. Am. Chem. Soc.* **2013**, *135*, 13737.

(3) Leuenberger, M. N.; Loss, D. *Nature* **2001**, *410*, 789.

(4) (a) Affronte, M.; Troiani, F.; Ghirri, A.; Condini, A.; Evangelisti, M.; Corradini, V.; Carretta, S.; Santini, P.; Amoretti, G.; Tuna, F.; Timco, G.; Winpenny, R. E. P. *J. Phys. D: Appl. Phys.* **2007**, *40*, 2999. (b) Stamp, P. C. E.; Gaita-Ariño, A. *J. Mater. Chem.* **2009**, *19*, 1718. (c) Troiani, F.; Affronte, M. *Chem. Soc. Rev.* **2011**, *40*, 3119. (d) Aromí, G.; Aguilà, G. D.; Gamez, P.; Luis, F.; Roubeau, O. *Chem. Soc. Rev.* **2012**, *41*, 537.

(5) (a) Christou, G.; Gatteschi, D.; Hendrickson, D. N.; Sessoli, R. *MRS Bull.* **2000**, *25*, 66. (b) Shatruk, M.; Avendaño, C.; Dunbar, K. R. In *Prog. Inorg. Chem.*; John Wiley & Sons, Inc., 2009; pp 155−334. (c) Rinehart, J. D.; Long, J. R. *Chem. Sci.* **2011**, *2*, 2078. (d) Layfield, R. A. *Organometallics* **2014**, *33*, 1084. (e) Pedersen, K. S.; Bendix, J.; Clérac, R. *Chem. Commun.* **2014**, *50*, 4396.

(6) (a) Schlegel, C.; van Slageren, J.; Manoli, M.; Brechin, E. K.; Dressel, M. *Phys. Rev. Lett.* **2008**, *101*, 147203. (b) Takahashi, S.; van Tol, J.; Beedle, C. C.; Hendrickson, D. N.; Brunel, L.-C.; Sherwin, M. S. *Phys. Rev. Lett.* **2009**, *102*, 087603. (c) Takahashi, S.; Tupitsyn, I. S.;

van Tol, J.; Beedle, C. C.; Hendrickson, D. N.; Stamp, P. C. E. *Nature* **2011**, *476*, 76.
(7) Hartke, K.; Kissel, T.; Quante, J.; Matusch, R. *Chem. Ber.* **1980**, *113*, 1898.
(8) Matsuda, F.; Tamura, H.; Matsubayashi, G. *Inorg. Chim. Acta* **1999**, *295*, 239.
(9) Dai, D.; Xiang, H.; Whangbo, M.-H. *J. Comput. Chem.* **2008**, *29*, 2187.
(10) Fukui, K.; Kojima, N.; Ohya-Nishiguchi, H.; Hirota, N. *Inorg. Chem.* **1992**, *31*, 1338.
(11) Abragam, A.; Bleaney, B. *Electron Paramagnetic Resonance of Transition Ions*; Oxford University Press: Oxford, 1970.
(12) Shores, M. P.; Sokol, J. J.; Long, J. R. *J. Am. Chem. Soc.* **2002**, *124*, 2279.
(13) The largest reported negative D detected by EPR is $-120 > D > -180$ cm^{-1}: Ruamps, R.; Maurice, R.; Batchelor, L.; Boggio-pasqua, M.; Guillot, R.; Barra, A. L.; Liu, J.; Bendeif, E.-E.; Pillet, S.; Hill, S.; Mallah, T.; Guihéry, N. *J. Am. Chem. Soc.* **2013**, *135*, 3017.
(14) Carlin, R. L. *Magnetochemistry*; Springer: New York, 1986.
(15) Gatteschi, D.; Sessoli, R. *Angew. Chem., Int. Ed.* **2003**, *42*, 268.
(16) (a) Meihaus, K. R.; Long, J. R. *J. Am. Chem. Soc.* **2013**, *135*, 17952. (b) McHugh, S.; Sarachik, M. P. *Mod. Phys. Lett. B* **2011**, *25*, 1795. (c) Sarachik, M. Magnetic Avalanches in Molecular Magnets. In *Molecular Magnets: Physics and Applications*; Batolome, J., Luis, F., Fernandez, J. F., Eds.; Springer: New York, 2014.
(17) (a) Schenker, R.; Leuenberger, M. N.; Chaboussant, G.; Loss, D.; Güdel, H. U. *Phys. Rev. B* **2005**, *72*, 184403. (b) Lopez, N.; Prosvirin, A. V.; Zhao, H.; Wernsdorfer, W.; Dunbar, K. R. *Chem.—Eur. J.* **2009**, *15*, 11390. (c) Meihaus, K. R.; Rinehart, J. D.; Long, J. R. *Inorg. Chem.* **2011**, *50*, 8484.
(18) Sessoli, R.; Caneschi, A.; Gatteschi, D.; Sorace, L.; Cornia, A.; Wernsdorfer, W. *J. Magn. Magn. Mater.* **2001**, *226−230*, 1954.
(19) Gómez-Coca, S.; Urtizberea, A.; Cremades, E.; Alonso, P. J.; Camón, A.; Ruiz, E.; Luis, F. *Nat. Commun.* **2014**, *5*, 4300 DOI: 10.1038/ncomms5300.
(20) Atanasov, M.; Zadrozny, J. M.; Long, J. R.; Neese, F. *Chem. Sci.* **2013**, *4*, 139.
(21) (a) Lucaccini, E.; Sorace, L.; Perfetti, M.; Costes, J.-P.; Sessoli, R. *Chem. Commun.* **2014**, *50*, 1648. (b) Pedersen, K. S.; Ungur, L.; Sigrist, M.; Sundt, A.; Schau-Magnussen, M.; Vieru, V.; Mutka, H.; Rols, S.; Weihe, H.; Waldmann, O.; Chibotaru, L. F.; Bendix, J.; Dreiser, J. *Chem. Sci.* **2014**, *5*, 1650.
(22) (a) Branzoli, F.; Carretta, P.; Filibian, M.; Zoppellaro, G.; Graf, M. J.; Galan-Mascaros, J. R.; Fuhr, O.; Brink, S.; Ruben, M. *J. Am. Chem. Soc.* **2009**, *131*, 4387. (b) Zadrozny, J. M.; Xiao, D. J.; Long, J. R.; Atanasov, M.; Neese, F.; Grandjean, F.; Long, G. J. *Inorg. Chem.* **2013**, *52*, 13123.
(23) (a) Zadrozny, J. M.; Liu, J.; Piro, N. A.; Chang, C. J.; Hill, S.; Long, J. R. *Chem. Commun.* **2012**, *48*, 3927. (b) Vallejo, J.; Castro, I.; Ruiz-Garcia, R.; Cano, J.; Julve, M.; Lloret, F.; De Munno, G.; Wernsdorfer, W.; Pardo, E. *J. Am. Chem. Soc.* **2012**, *134*, 15704. (c) Colacio, E.; Ruiz, J.; Ruiz, E.; Cremades, E.; Krzystek, J.; Carretta, S.; Cano, J.; Guidi, T.; Wernsdorfer, W.; Brechin, E. *Angew. Chem., Int. Ed.* **2013**, *52*, 9130.
(24) (a) Mitrikas, G.; Sanakis, Y.; Raptopoulou, C. P.; Kordas, G.; Papavassiliou, G. *Phys. Chem. Chem. Phys.* **2008**, *10*, 743. (b) Timco, G. A.; Faust, T. B.; Tuna, F.; Winpenny, R. E. P. *Chem. Soc. Rev.* **2011**, *40*, 3067. (c) Yang, J.; Wang, Y.; Wang, Z.; Rong, X.; Duan, C.-K.; Su, J.-H.; Du, J. *Phys. Rev. Lett.* **2012**, *108*, 230501. (d) Warner, M.; Din, S.; Tupitsyn, I. S.; Morley, G. W.; Stoneham, A. M.; Gardener, J. A.; Wu, Z.; Fischer, A. J.; Heutz, S.; Kay, C. W. M.; Aeppli, G. *Nature* **2013**, *503*, 504.
(25) Horvath, B.; Möseler, R.; Horvath, E. G. *Z. Anorg. Allg. Chem.* **1979**, *450*, 165.
(26) Hansen, T. K.; Becher, J.; Jorgensen, T.; Varma, K. S.; Khedekar, R.; Cava, M. P. *Org. Synth.* **1996**, *73*, 270.
(27) Varma, K. S.; Bury, A.; Harris, N. J.; Underhill, A. E. *Synthesis* **1987**, *9*, 837.
(28) Harrison, W. T. A.; Howie, R. A.; Wardell, J. L.; Wardell, S. M. S. V.; Comerlato, N. M.; Costa, L. A. S.; Silvino, A. C.; de Oliveira, A. I.; Silva, R. M. *Polyhedron* **2000**, *19*, 821.
(29) Bain, G. A.; Berry, J. F. *J. Chem. Educ.* **2008**, *85*, 532.
(30) *APEX2*, v. 2009; Bruker Analytical X-Ray Systems, Inc: Madison, WI, 2009.
(31) Sheldrick, G. M. *SADABS*, version 2.03; Bruker Analytical X-ray Systems, Inc: Madison, WI, 2000.
(32) Sheldrick, G. M. *SHELXTL*, version 6.12; Bruker Analytical X-ray Systems, Inc: Madison, WI, 2000.
(33) Farrugia, L. J. *J. Appl. Crystallogr.* **1999**, *32*, 837−838.
(34) Hassan, K.; Pardi, L. A.; Krzystek, J.; Sienkiewicz, A.; Goy, P.; Rohrer, M.; Brunel, L. C. *J. Magn. Reson.* **2000**, *142*, 300.
(35) Stoll, S.; Schweiger, A. *J. Magn. Reson.* **2006**, *178*, 42.